Marine Ecology. ISSN 0173-9565

ORIGINAL ARTICLE

Reproductive output in a Mediterranean population of the homosclerophorid *Corticium candelabrum* (Porifera, Demospongiae), with notes on the ultrastructure and behavior of the larva

Manuel Maldonado & Ana Riesgo

Department of Marine Ecology, Centro de Estudios Avanzados de Blanes (CSIC), Girona, Spain

Keywords
Ciliary rootlets; gastrulation; invertebrate reproduction; recruitment; sponges; tight junctions.

Correspondence
Manuel Maldonado, Department of Marine Ecology, Centro de Estudios Avanzados de Blanes (CSIC), Acceso Cala St Francesc 14, Blanes 17300, Girona, Spain.E-mail: maldonado@ceab.csic.es

Accepted: 22 April 2008

doi:10.1111/j.1439-0485.2008.00244.x

Abstract

The reproductive output of sponges possessing small elusive larvae remains little investigated, even though they are relevant community members in many cases. This makes difficult to understand their life cycles and population dynamics. In this study we monitored the dynamics of embryogenesis and larval output in a north-western Mediterranean population of the sublittoral demosponge *Corticium candelabrum*. The sponge was moderately abundant, mostly concentrated at overhangs and shaded walls. The population was dominated by relatively small individuals, averaging 1.26 cm^3 in size. About 89% of individuals in the population produced gametes. Body size did not preclude reproduction, as gametes and embryos occurred in sponges ranging from 0.24 to 13.5 cm^3 in size. On average, individuals produced 21.3 ± 12 embryos per mm^3 of sponge tissue, but inter-annual variability in the reproductive effort was noticed. Larval release was asynchronous at both the individual and the population level, with sponges releasing larvae from early July to August. A yearly production was estimated of about half a million larvae per m^2 of rocky bottom at those sites where this species occurs. Living larvae measured 340 ± 25 μm in length, were bulb-shaped, entirely ciliated, and swam with a clockwise rotation. They were hollow, with an internal cavity limited by a monolayered epithelium of columnar cells. All larval cells had a distal cilium arising from a principal centriole connected to a basal foot. There was an orthogonal accessory centriole giving rise to a short striated rootlet (21-nm periodicity band) that ran between the nucleus and the Golgi apparatus. This is the first reported case in Porifera of a ciliary rootlet derived from an accessory centriole, an uncommon arrangement also found in choanoflagellates. Despite sharing many features, cells of the anterior, medial, and posterior larval region were easily distinguishable from each other because of differences in their internal organization and yolk content. At the distal and proximal poles of all cells, the plasmalemma thickened to produce special junctions and seal the larval epithelium. Distal junctions were septate. The larval cavity was filled with vertically transmitted symbiotic bacteria and collagen fibrils. Collagen condensed below the larval epithelium at different degrees, but was absent in some areas, raising doubts about the occurrence of a true basement membrane. Larvae showed neither recognizable photoreceptory organelles nor evident behavioral responses to experimental light cues. Because the high larval production does not mirror adult abundance in the community, we suspect high

levels of larval losses during dispersal and elevated impact of post-settlement mortality as the probable result of unselective settlement at unsuitable sites.

Problem

Demosponges make up the largest class of the phylum Porifera, comprising about 6000 described species (Hooper & Van Soest 2002). The homosclerophorids are a distinct group within the demosponges, consisting of just six genera and about 60 valid species (Muricy & Díaz 2002). Members of two genera do not secrete siliceous spicules, whereas the remaining species produce a variety of small bi-rayed, three-rayed and/or tetra-rayed (microcalthrops) silica spicules. At the beginning of the 20th century, the microcalthrops of homosclerophorids were postulated to be the ancestral spicule type from which the remaining spicule types of other siliceous sponges derived (Dendy 1921), a hypothesis that has been neither validated nor refuted to date. A recent histological study has also revealed that some homosclerophorids appear to be able to secrete spicules within the epithelial cells, a unique pathway of spicule production in the Porifera (Maldonado & Riesgo 2007). Distinctive features of homosclerophorids are also the possession of an evident basement membrane of type IV collagen below their epithelia (Boute *et al.* 1996) and a spermatogenesis developing through a maturation gradient within the spermatic cysts to produce spermatozoa having a C-shaped acrosome (Baccetti *et al.* 1986; Boury-Esnault & Jamieson 1999; Riesgo *et al.* 2007a).

The homosclerophorid sponges are currently at the centre of an intense phylogenetic debate. Analysis of the complete mitochondrial genome of a homosclerophorid (Wang & Lavrov 2007) revealed many features that do not occur in other demosponges, suggesting this group to be phylogenetically located near the base of Demospongiae. In contrast, studies based on rRNA indicated that the Homosclerophorida appear to have more affinity with Calcarea than with any other demosponge group (*e.g.* Borchiellini *et al.* 2004; Nichols 2005) and could represent a fourth major evolutionary clade within the Porifera. Because rRNA and mtDNA data analyses provide conflicting phylogenetic signals, morphological features that are expected to contain additional phylogenetic information to clarify the origin and/or relationships of this sponge clade are attracting much interest. Although much work on this issue has been done in the group, much is still to be done. For instance, although a basement membrane has usually been reported below both the choanoderm and pinacoderm of most homosclerophorids studied so far (Muricy & Díaz 2002), in some species (*e.g. Corticium candelabrum*) a basement membrane is only evident below the choanocytes, not underneath the exo- and endo-pinacocytes (*e.g.* Maldonado & Riesgo 2007). Likewise, it is often generalized that pinacocytes of homosclerophorids are monociliated cells (*e.g.* Muricy & Díaz 2002). Nevertheless, although this pattern is seen in some genera (*e.g. Plakina*: Muricy *et al.* 1999), others (*e.g. Corticium*: Maldonado & Riesgo 2007) appear to have only ciliated endopinacocytes and unciliated exopinacocytes through most of the sponge external surface. Thus, the real phylogenetic significance of the variability in these assumedly distinctive features remains little understood in the absence of further research. Additional detailed studies based on year-round sampling are required to elucidate whether the Homosclerophorida could also be characterized by a peculiar pattern of oogenesis. A recent study in the species *C. candelabrum* (Riesgo *et al.* 2007a) has reported that despite larval release occurring just once a year, production of new oocytes takes place every single month. It is unclear the extent to which this pattern occurs in the group.

Controversy also exists regarding the interpretation of embryo development in the group, a process through which the solid late-stage blastula gives rise to a hollow larva. The centrifugal migration of the internal blastomeres to form the hollow embryo has been interpreted by some authors as a process by which a solid blastula forms a subsequent hollow blastula stage that corresponds to the larva, called 'cinctoblastula' (*e.g.* Ereskovsky & Boury-Esnault 2002; Boury-Esnault *et al.* 2003). The founders of this 'school' never declare when the hollow larva – which is regarded as a blastula stage – gastrulates; they report the larva to settle and metamorphose into the early juvenile (=rhagon), apparently without going through such an embryonic process (Ereskovsky *et al.* 2007). The alternative view is that a gastrulation by centrifugal cell migration takes place after cleavage – just like in the remaining Metazoa – producing a hollow gastrula, which is the larval stage (Maldonado 2004).

In addition to embryo development, the morphological features of the larval stage itself are worthy of attention and further research. Of the five different larval types described in Demospongiae so far (Maldonado & Bergquist 2002; Maldonado 2006), one is exclusive to the Homosclerophorida. Different morphological and cytological aspects of embryos and larvae had been described

for members of the genera *Oscarella* (=*Octavella*), *Plakina*, *Corticium*, and *Pseudocorticium* (*e.g.* Barrois 1876; Schulze 1880; Heider 1886; Meewis 1938; Lévi & Porte 1962; Tuzet & Paris 1964; Bergquist *et al.* 1979; Boury-Esnault *et al.* 2003; De Caralt *et al.* 2007). Comparatively, there is far less work reporting data on the swimming behavior of the free-swimming larva (*e.g.* Bergquist *et al.* 1979; Boury-Esnault *et al.* 2003), a situation in part justified by its relatively small size, which hinders collection of free larvae in the field. The few available data are not exempt from conflict. For example, whereas the larva of *Oscarella* has been reported to swim with a clockwise rotation by Bergquist *et al.* (1979), the larva of *Plakina* has been described as a crawling larva with counter-clockwise rotation by the same author (Bergquist *et al.* 1979) and, additionally, as a swimming larva with a clockwise rotation by other authors (Boury-Esnault *et al.* 2003). Research on larval output and behavior is also required to explain ecological distribution patterns in this group, whose members are common in many sublittoral temperate and tropical communities.

In this study, we have monitored the brooding process of the species *Corticium candelabrum* Schmidt, 1862 in an attempt to estimate larval outputs and predict timing of release. We have also collected some free-swimming larvae from the field and described basic swimming behavior. The objective of this research was to provide basic information on the reproductive output to facilitate subsequent population studies on dispersal and early recruitment processes. Additionally, given that the ultrastructural information is emerging as a crucial tool to complement molecular approaches in the inference of the phylogenetic relationships of the homosclerophorids, we have conducted a histological study of this larva, also recently investigated by Boury-Esnault *et al.* (2003) and De Caralt *et al.* (2007). The cell re-organizations documented during embryogenesis and the novel ultrastructural larval traits found in this study are discussed in a context intended to be applicable to an audience interested in phylogenetic inference.

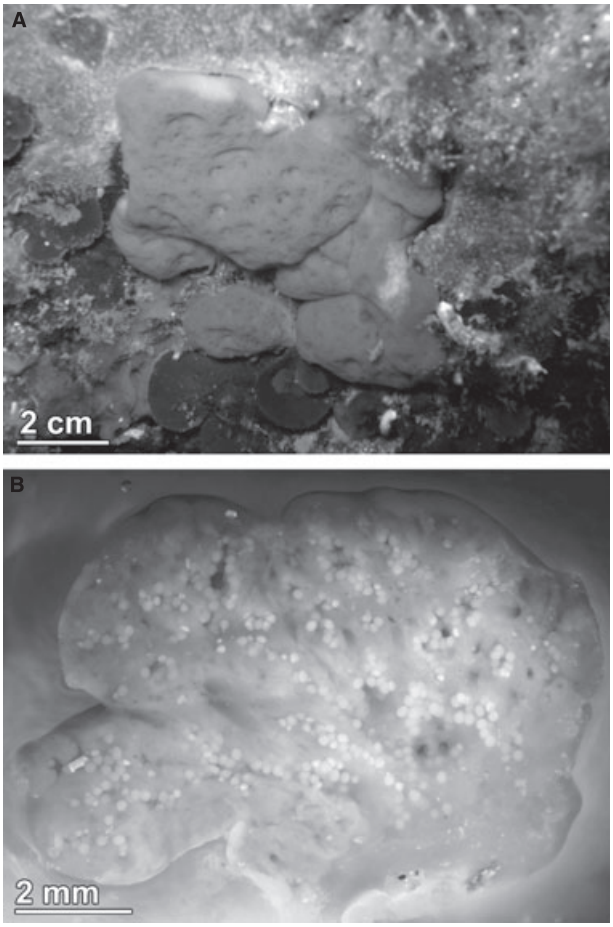

Fig. 1. (A) Individual of *Corticium candelabrum* growing in an overhang at a depth of 8 m. Note occurrence of red algae *Peyssonnelia* and other organisms well adapted to shaded habitats. (B) Hand section of individual no. 7 showing whitish spheres that are late embryos in the tissue.

Material and Methods

Study species

There is controversy about whether *C. candelabrum* is a cosmopolitan species or a Mediterranean endemism, although the latter appears to be more likely (Muricy & Díaz 2002). The Mediterranean *C. candelabrum* individuals are small, orangish-brown, cushion-shaped to lobed sponges, measuring up to 1.5 cm in thickness and 15 cm in the largest diameter (Fig. 1A). The studied population of *C. candelabrum* occupies the 5–20 m depth range. The sponge is a typical member of communities characterized by semisciaphilic organisms (*e.g.* Ros *et al.* 1985), which develops on the walls of the sublittoral rocky cliff in the north Catalan coast (Spain, northwestern Mediterranean) between Blanes (2°48.12′ N, 41°40.33′ E) and Tossa de Mar (2°54′55.77″ N, 41°42′33.25″ E).

Embryo abundance and larval output

For long-term monitoring of reproductive activity in the population, we tagged five large and presumably mature individuals at random; these were sampled monthly, from October 2003 to October 2005. We collected a small tissue piece (approximately $1 \times 0.5 \times 0.5$ cm) from each sponge at each sampling time by SCUBA diving and using surgical scissors. In no case did tissue collection cause the death of the sampled sponges or perceivable functional damage.

When samples from the tagged individuals revealed that the abundance of zygotes and early embryos was about to peak in the population, which happened in summer, we increased both the sampling frequency (10-day intervals) and the number of sampled individuals (n = 30). At each time of 'summer sampling' we collected tissue pieces from the five tagged individuals, as well as from 25 non-tagged sponges at random, irrespective of whether they had been sampled in a previous dive.

Tissue samples for light microscopy were maintained in ambient seawater for transportation to the laboratory (1–2 h) and fixed in 4% formaldehyde in seawater for 24 h. Samples were then desilicified with 5% hydrofluoric acid for 1.5 h, rinsed in distilled water, dehydrated through a graded ethanol series (70%, 96%, 100%), cleared in toluene, and embedded in paraffin to cut them into 5-μm-thick sections using an 2040 Autocut Reichert-Jung microtome. After deparaffination with xylene, sections were stained with Hematoxylin-PAS and observed through a Zeiss Axioplan II compound microscope connected to a Spot Cooled Color digital camera. To count pre-gastrular (solid) embryos and post-gastrular (hollow) embryos per tissue volume, we took three pictures (×100) of each of two non-serial sections per individual. Likewise, pictures of tissue were taken at least 240 μm from each other to avoid overlapping of embryos leading to overestimation. The four pictures provided a total surveyed area of 7 mm^2 per individual. By studying sections obtained from the five tagged individuals, we estimated average density (mean number of embryos per mm^3) of pre-gastrular and post-gastrular embryos over time. Additionally, we used the set of samples provided by the 30 individuals selected at random (June 25, July 1, July 13, July 22, August 3, and August 11, 2004) to obtain a more accurate estimate of the percentage of reproductive individuals in the population, as well as to identify the moment of maximum average density of embryos in the sponge tissue immediately prior to larval release. To estimate the number of embryos per mm^3, we followed the formula proposed by Elvin (1976):

$$E = (N \cdot (t/(d + t)) \cdot F,$$

where E is number of embryos per mm^3, N is the number of embryos counted in the 7-mm^2 field of the histological sections, t is the thickness of the section (5 μm), D is the average diameter of embryos (170 μm), and F (=28.5) is a factor converting the volume of observation to 1 mm^3.

When the histological sections indicated a decrease in the density of post-gastrular embryos, we monitored sponges in the field for larval release during both morning dives (usually between 10:00 and 13:00 GMT) and night dives (usually between 21:30 and 23:00 GMT). Because incident light often makes sponge larvae brighter, we assumed that, in the case of night-time release, the use of powerful flashlights would guarantee their visualization. When free-swimming larvae were encountered, we collected them using plastic syringes for further behavioral and histological observations.

During each sampling, we measured seawater temperature (±0.5 °C) at the sponge habitat using an underwater thermometer (Suunto). The relationship between temperature and embryogenesis was examined by plotting monthly temperature values *versus* estimated density (abundance per mm^3) of pre-gastrular and post-gastrular embryos.

To estimate larval output at the population level, we first conducted field estimates of sponge abundance using 50 × 50 cm PVC quadrats (n = 498) and measured the volume of each individual (n = 497) found in the quadrats. A gross estimate of volume for this cushion-shaped to moderately lobate (Fig. 1) sponge was obtained by using a ruler and approximating the shape of their entire body or that of their respective lobes to known geometrical figures (sphere, prolate spheroids, cylinder, *etc.*). Because preliminary surveys revealed a very irregular spatial distribution, we sampled three different subpopulations: St Anna Point, 41°40′23″ N, 02°48′14″ E; St Francesc Point, 41°40′36″ N, 02°48′34″ E; and Moro Point, 41°42′02″ N, 02°54′52″ E. Two divers inspected about 500 m^2 of community at each of the three sites, placing the quadrats randomly to examine a total area of 124.5 m^2 (= 498 quadrats). We finally tested differences in sponge abundance and sponge size as a function of site and light exposure of habitat (shaded habitats: north-facing and overhangs *versus* well-lit habitats: south-facing walls and moderately sloping rocky bottoms) using a two-way ANOVA. Nevertheless, sponges occurred at well-lit habitats in only one of the three studied sites and did so with very low abundance. Therefore, although we considered the data provided from the few sponges growing in well-lit habitats, the 'light-exposure' factor was eliminated from the ANOVA analysis of sponge abundance and size, which finally became a Kruskal–Wallis one-way analysis of variance on ranks, as the many empty quadrats meant that the data were not homoscedastic.

We estimated average larval output per m^2 of community by considering total sponge volume per quadrat and average embryo density per cm^3 of sponge tissue (as estimated on July 1, immediately prior to the onset of larval release). We also examined the relationship between sponge size and sexual maturity by collecting tissue pieces of individuals (n = 25) that spanned a large size range during May 2007 and checking them for gametes and/or embryos through a dissecting microscope.

On the few occasions in which free-swimming larvae were collected (n = 5), they were placed in 50-ml Petri dishes and monitored under the dissecting microscope for

3 h. We documented their swimming behavior and performed a preliminary examination of their photoresponse under diverse light conditions, although the low number of collected larvae did not allow the behavioral experimentation to be replicated.

Histological and cytological observations

Histological sections for assessment of embryo abundance during 2004 and 2005 were also used to investigate the process of cleavage and subsequent embryo development under a Zeiss Axioplan II compound microscope provided with phase contrast objectives and connected to a digital camera.

Transmission electron microscopy (TEM) was used to describe the ultrastructure of free-swimming larvae. Three larvae were fixed within 3 h after collection, according to the protocol detailed elsewhere (Maldonado *et al.* 2005). Primary fixation was in 2.5% glutaraldehyde in 0.2 M Millonig's phosphate buffer (MPB) and 1.4 M sodium chloride for 1 h. Samples were then rinsed with MPB for 40 min, post-fixed in 2% osmium tetroxide in MPB, dehydrated in a graded acetone series, and embedded in Spurr's resin. Ultrathin sections obtained with an Ultracut Reichert-Jung ultramicrotome were mounted on formvar-coated gold grids and stained with 2% uranyl acetate for 30 min, and then with lead citrate for 10 min (Reynolds 1963). Observations were conducted with a JEOL 1010 transmission electron microscope (TEM) operating at 80 kV and provided with a Gatan module for acquisition of digital images.

Results

Dynamics of embryogenesis and larval release

Examination of histological sections from 149 individuals of *C. candelabrum* confirmed that 89% of the sampled individuals produced gametes and embryos. Those individuals (11%) that did not contain embryos were consistently of small size (<1 cm^3). In the 2 years of study, embryogenesis coincided with the seasonal water warming (mid March) and extended for several months (Fig. 2A). Production of pre-gastrular embryos rapidly increased with increasing temperatures in spring. In the tagged sponges, the maximum density of embryos (pre-gastrular and post-gastrular pooled) was attained in the first week of July in 2004, reaching a value of 27.3 ± 12.5 embryos·mm^{-3} (Fig. 2A). In 2005, the maximum density took place during the last week of May, reaching a value of just 15.3 ± 8.8 embryos·mm^{-3}. These results reveal important inter-annual variability in the reproductive effort. Pooling data from 2004 and 2005 for the five tagged individuals, the maximum density averaged 21.3 ± 12 embryos·mm^{-3}. This value was very close to the density figure (18.9 ± 15.4; Fig. 2B) obtained by examining tissue samples of 30 individuals sampled at random during the first week of July 2004 – immediately before the onset of larval release in the population.

An inflection in the mean density of post-gastrular embryos (Fig. 2A) indicated that larval release started sometime in July in both years and that it extended, at the population level, for several weeks, coinciding with the period of maximum seawater temperatures (late July to mid August). Late-stage embryos looked whitish while they were brooded in the maternal tissue (Fig. 1B), but they became brownish upon release.

Massive larval release by *C. candelabrum* individuals was never seen during the many dives that we completed in summer 2004 and 2005. In some morning dives, we occasionally noticed an isolated, tiny larva coming out in the exhalant water jets of some individuals.

To estimate larval output in the local population, we counted the number of sponge individuals in each 2500-cm^2 quadrat of the rocky-bottom community (n = 498) and estimated the size of each individual (n = 497). The

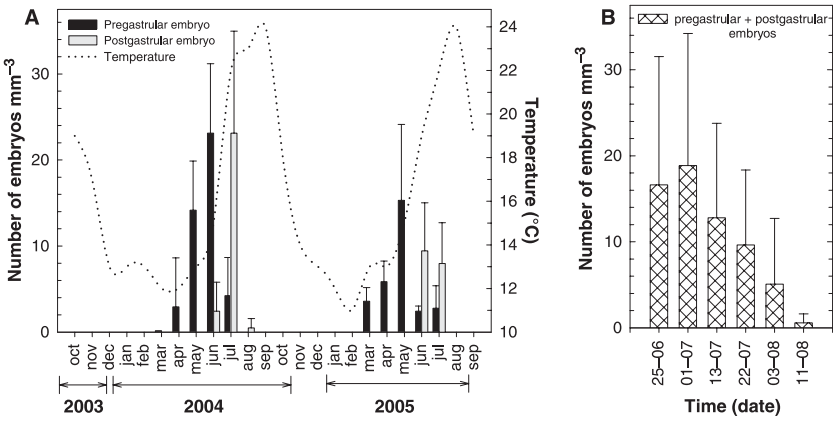

Fig. 2. (A) Mean density (± SD) of embryos (pre-gastrulated and post-gastrulated) in the sponge tissue of five tagged individuals over a biannual cycle (October 2003 to September 2005). Temperature is plotted on a second axis. (B) Density of embryos in the sponge tissue of 30 sponges taken at random at each sampling during the peak of embryogenesis and larval release in summer 2004.

distribution of the individuals was extremely patchy. Sponges occurred at similar densities at the three studied sites, according to the Kruskal–Wallis tests ($P = 0.716$; Fig. 3A). In all three sites, they were considerably more abundant in quadrats located on shaded vertical walls and overhangs than at moderately sloping substrata and south-facing, well-lit rocky walls (Fig. 3A). The average number of individuals per quadrat in shaded habitats was 1.5 ± 3.5, whereas it was just 0.1 ± 0.6 at illuminated, south-facing walls. Indeed, sponges grew exposed to light in only one of the three subpopulations studied, and this happened in very few cases (Fig. 3A). Measurement of a total of 497 individuals, ranging in size from 0.04 to 58.4 cm^3, revealed that population size distribution was not normal but was characterized by an overabundance of small sponges (Fig. 4). The total sponge volume per quadrat (Fig. 3B) and average sponge size per quadrat (Fig. 3C) tended to be higher in Moro subpopulations than in the two other sites. Nevertheless, a Kruskal–Wallis test revealed that such differences were not statistically significant ($P = 0.249$ for total volume per quadrat; $P = 0.129$ for average individual volume per quadrat), since, although the largest specimens occurred at the former site, small individuals were also very abundant. In shaded habitats, total sponge volume per quadrat and mean individual size per quadrat averaged 10.5 ± 37.5 and 2.1 ± 6.2 cm^3, respectively. These figures dropped drastically in well-lit habitats, being 1.3 ± 11 and 0.4 ± 2.5, respectively. At the population level, individual body size averaged 1.2 ± 4.8 cm^3. A small body size did not preclude production of sexual products, as gametes were found in all 25 individuals selected at random from the population, even when their size was 0.24–13.5 cm^3 (Fig. 5). Considering that the average total sponge volume per quadrat was 5.96 ± 28 cm^3 and the average embryo density in the sponge tissue prior to larval release was 21.3 ± 12 embryo·mm^{-3}, we estimated that about 507,000 larvae ($= 4 \times 5.96 \times 21{,}300$) are released on average per m^2 of rocky bottom at those sites where this species occurs.

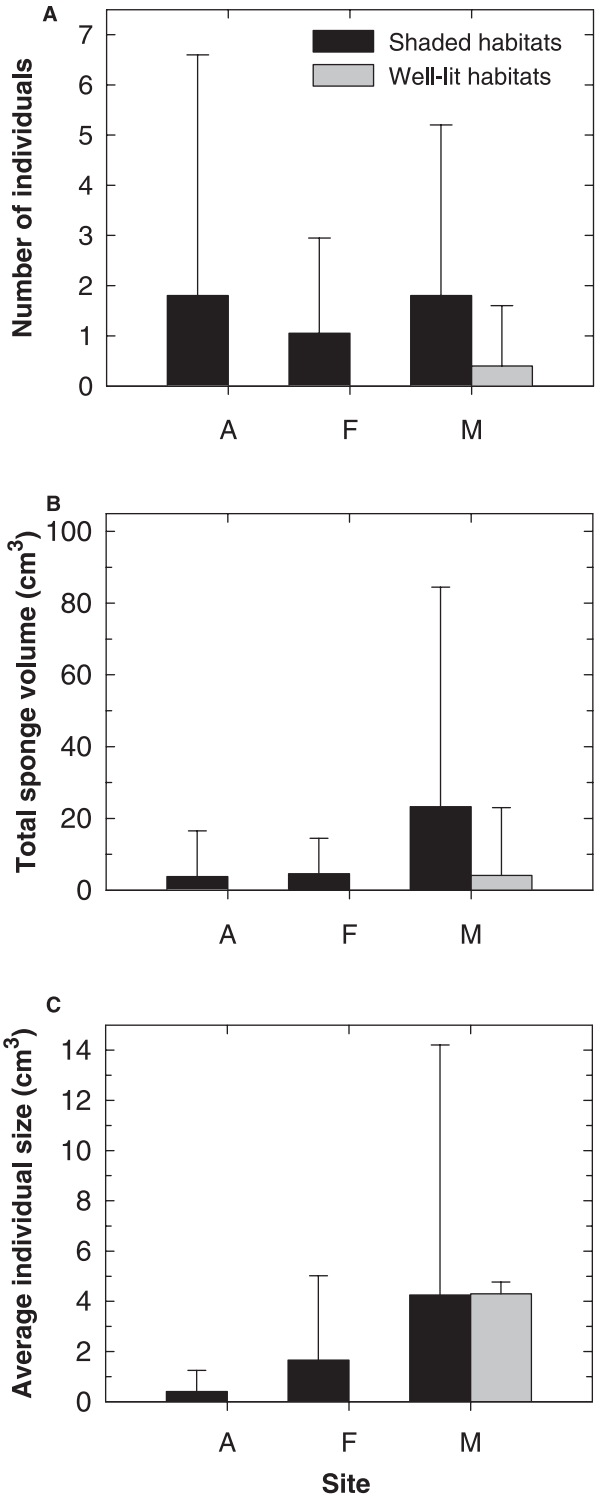

Fig. 3. (A) Mean number of individuals (± SD), (B) total sponge volume (± SD), and (C) average individual size (± SD) of *Corticium candelabrum* per 2500 cm^2 sampling quadrat (n = 498) at shaded and well-lit habitats at the subpopulations of three different sites (A = Sta. Anna Point, F = St Francesc Point, M = Moro Point).

Larval shape and basic behavior

Upon leaving the exhalant water jets of their mother sponges, larvae slowly drifted with the anterior pole oriented upward and attaining no active horizontal displacement, entrapped by seawater viscosity. Only five larvae were successfully collected and taken alive to the laboratory. Living larvae measured 340 ± 25 μm in length and were bulb-shaped (Fig. 6A), with a clear anterior–posterior morphological axis. They had an inflated anterior portion (the one directed forward when larvae swim horizontally), which took up about two-thirds of the

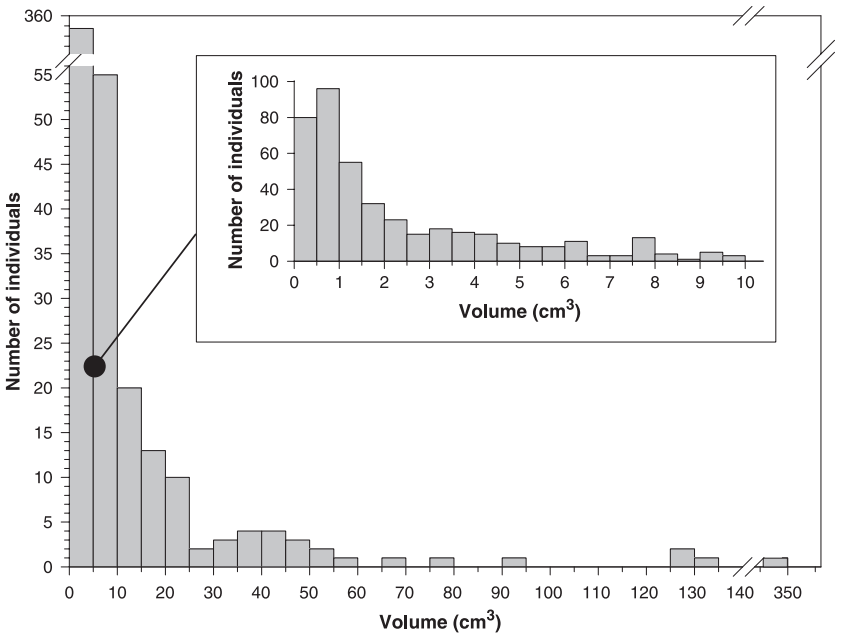

Fig. 4. Population size distribution of *Corticium candelabrum* estimated from 497 individuals measured at random. Because small individuals (<10 cm^3) dominated the population (n = 395), an inset is used to detail abundance of these individuals per 1-cm^3 size classes.

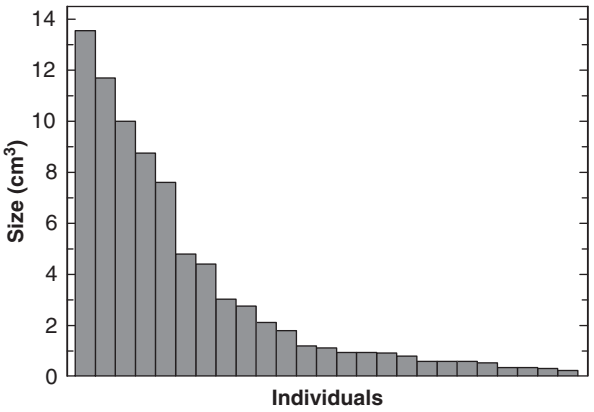

Fig. 5. Individuals (n = 25) collected at random from the population during May 2007, ordered by decreasing size and examined for gametes and/or embryos. All individuals, irrespective of size, contained embryos.

larval body and was separated from a narrower, blunt, posterior end by a thin medial constriction. The anterior portion was 275 μm in maximal diameter and the mid constriction was 230 μm. The larva was brownish, but the anterior portion was notably lighter than the posterior one. The larva was entirely ciliated. During light microscopy observation of living larvae, the cilia of the anterior portion looked longer (about 25 μm in length) than those of the posterior one (about 10 μm in length; Fig. 6A and B, but see Discussion for further interpretation of this apparent length difference). After fixation and embedding, the larval body became more streamlined, so that the anterior region became narrower and the medial constriction was barely perceptible (Fig. 6C). In these longitudinal histological sections, larvae measured up to 500 μm in length and 290 μm at the maximum diameter (Fig. 6C).

When larvae were placed in 50-ml Petri dishes with unfiltered seawater and examined under a dissecting microscope, they were seen to alternate drifting periods in a vertical position (like those observed in field conditions) with periods of active horizontal swimming. In both 'attitudes', larvae never stopped rotating around their longitudinal axis. Rotation was consistently clockwise when seen from the anterior pole. Because larvae showed no noticeable behavioral responses to changes in intensity of either natural light or artificial light sources during the first 3 h in laboratory conditions, and because the low numbers of collected larvae at each time consistently precluded appropriate replicable experimentation, we decided not to explore the larval photoresponse further. Therefore, all larvae were fixed for ultrastructural investigations after 3 h observation.

Embryo development and larval histology

The free-swimming larva was hollow despite originating from a solid blastula (stereoblastula; Fig. 7A,B). Hollowing took place at the late-stage blastula when the internal blastomeres migrated towards the periphery of the embryo. This centrifugal migration started simultaneously at several points (Fig. 7C), with blastomeres initially entering the nascent epithelium through many different points (Fig. 7D), then through only a few points (Fig. 7F), and finally at a single point (Fig. 7G). As soon as blastomeres entered the epithelium, they became

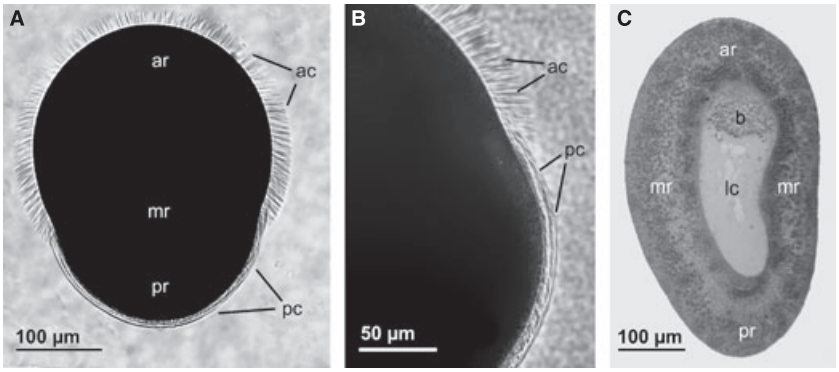

Fig. 6. Free-swimming larva of *Corticium candelabrum*. (A) General view showing the bulb shape of the larva, with a large anterior region (ar) separated from a smaller posterior region (pr) by a constriction at the medial region (mr). Note that the cilia of the anterior region (ac) look longer than those of the posterior region (pc) possibly because they are bent. (B) Detail of the medial region, showing a comparative view of anterior (ac) and posterior (pc) cilia of the larva. (C) Longitudinal section of the larva showing the three epithelial regions (ar, mr, pr) and the internal cavity (lc) filled with bacteria (b) that occur accumulated at the anterior pole (ar).

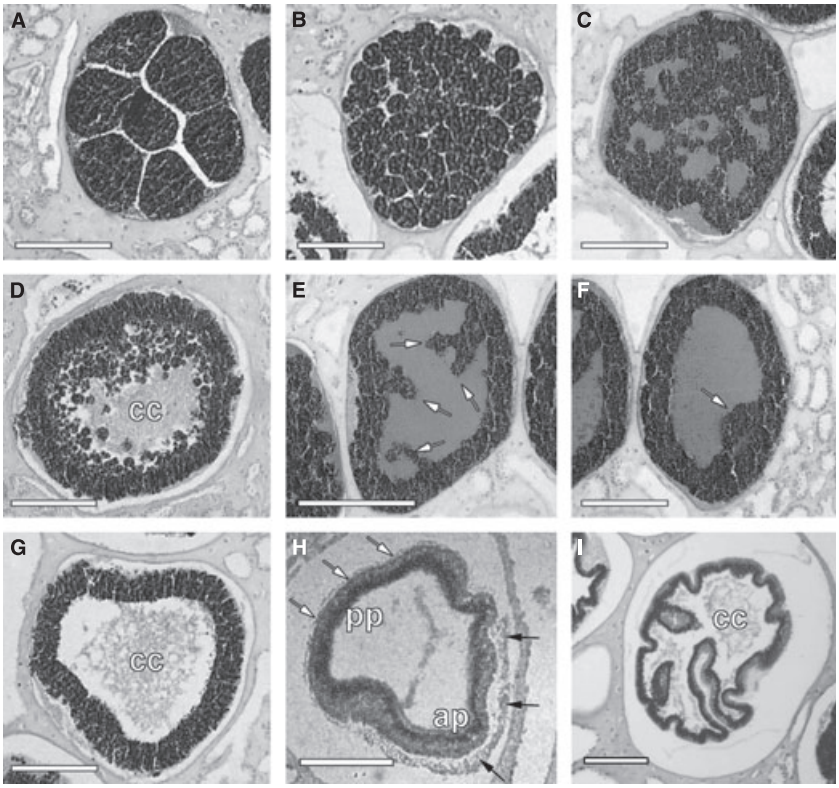

Fig. 7. Sequence of cell re-arrangements making the solid blastula become a hollow larva. (A) Early blastula. (B) Late-stage blastula. (C) Late-stage blastula in which the internal blastomeres initiated migration towards the periphery. (D) Late-stage blastula stage in which virtually all round blastomeres have migrated to the periphery and started incorporating massively at the nascent epithelium, becoming columnar epithelial cells. The lumen of nascent cavity has started being filled with material (cc) with strong affinity for hematoxylin, which was demonstrated by TEM to consist of symbiotic bacteria and collagen fibrils. (E,F) Late-stage blastulae in which the last blastomeres were migrating into to the nascent epithelium through just a few points (arrows) and, finally, through a single point (arrow). (G) Newly formed hollow embryo characterized by a columnar epithelium and a large cavity (cc) filled with symbiotic bacteria and collagen. (H) Embryo showing an early stage of epithelial convolution. Note that cilia (black arrows) at one of the embryo poles (ap) appear to project further from the epithelium than those (white arrows) at the opposite pole (pp). (I) Late-stage embryo immediately prior to being released as a free-swimming larva, in which the substantial folding of the epithelium denotes intense mitotic activity in the epithelial cells. Note also the content of the embryonic cavity (cc).

columnar cells that started secreting collagen fibrils (Fig. 7G) and developed a cilium (Fig. 7H). These epithelial cells subsequently divided by mitosis to increase their number and the extension of the larval epithelium, causing an epithelial folding (Fig. 7I) similar to that seen during formation of specialized cell layers in the morphogenesis of other invertebrates.

The internal cavity of the free-swimming larva was limited by a body wall consisting of a monolayered epithelium made of columnar cells that possess a distal cilium. The larva showed a macroscopic regionalization into anterior, medial and posterior regions, but cells of all three regions were similar in size (30–35 μm, in length and 1.9–2.4 μm in diameter) and all contained a nucleolate, ovoid nucleus of similar size (3.5–4.2 μm in length and 1.2–1.5 μm in maximum diameter). However, there were obvious differences in internal cell organization as a function of their topological location in the larval body, so that cells of the anterior, medial, and posterior regions were easily distinguishable from each others (Figs 8A, 9A and 10A).

Cells at the anterior region contained many very electron-dense yolk bodies, typically filling about two-thirds of their proximal cytoplasm (Fig. 8A). Yolk bodies were membrane-bound and had an evident paracrystalline substructure (Fig. 8B), which suggested a significant

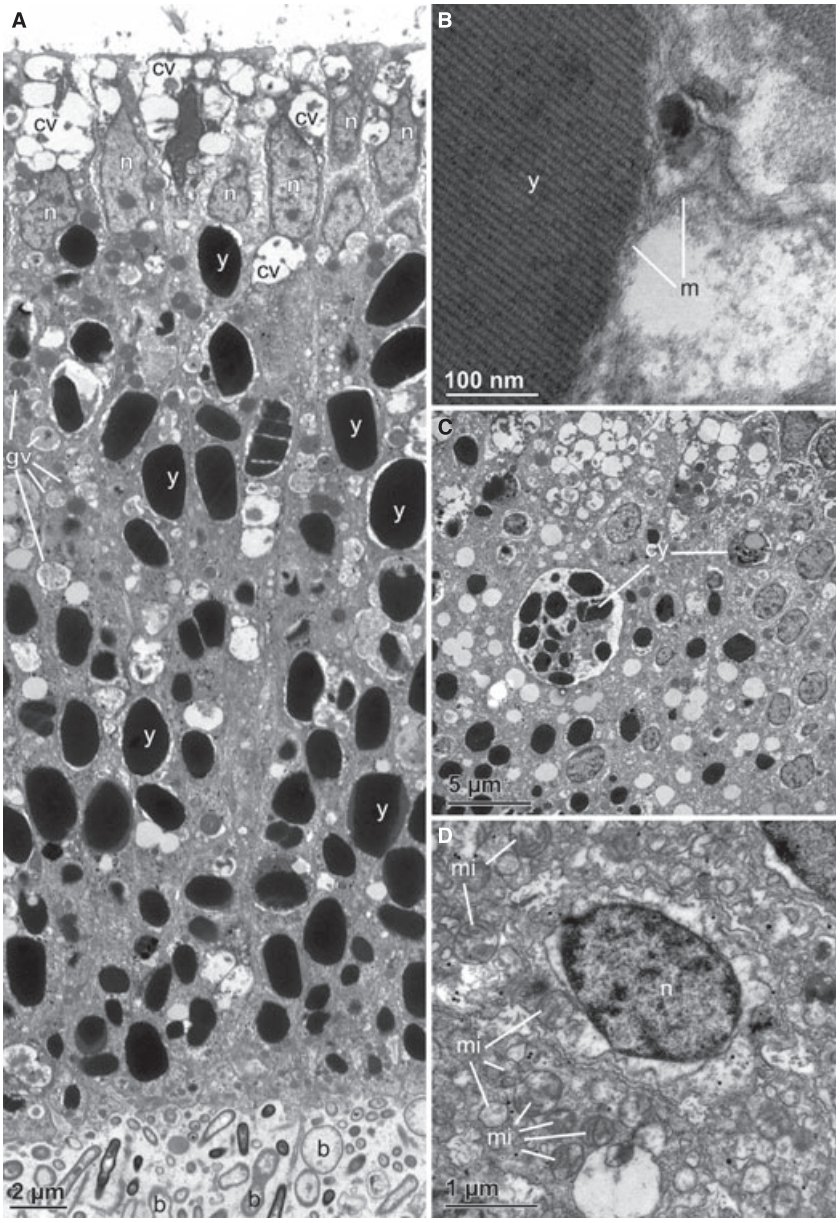

Fig. 8. Cells of the anterior larval region. (A) General view of entire cells at the anterior region, showing accumulation of electron-clear vesicles (cv) and the nucleolated nucleus (n) below the distal surface. Most of the cell is filled with yolk bodies (y) and diverse vesicles with granulose contents (gv). The proximal cell surface delimits the internal cavity, which is filled with bacteria (b) and collagen fibrils. (B) Detail of a yolk body (y) showing its paracrystalline structure and the surrounding membrane (m). (C) Details of two complex membrane-bound yolk inclusions (cy) containing a combination of simpler yolk bodies, granulose vesicles, and lipid droplets. (D) Detail of the nucleus (n) and the surrounding cytoplasm containing abundant small mitochondria (mi).

proteinaceous composition. There were also occasional membrane-bound complex inclusions, which combined yolk bodies with granulose material and lipid droplets (Fig. 8C). The distal cytoplasm was characterized by numerous vesicles with either electron-clear or granulose content, which occupied about one-third of the cell length (Fig. 8A). Many of the distal vesicles appeared to be fusing with each other, and also with the cell membrane, as if they were releasing their content to the external ciliated surface of the larva. Nevertheless, neither an evident mucous layer nor a well-developed glycocalyx was observed on the distal surface of ciliated cells. The nucleolate nucleus was consistently located at a subdistal position, surrounded by numerous small mitochondria (Fig. 8D). The nucleus separated the narrow band of distal cytoplasm filled with electron-clear vesicles from the larger proximal region filled with the very electron-dense yolk bodies (Fig. 8A).

At the mid region of larval epithelium, there was a 50–65-μm-wide, belt-like band made up of 29–36 cells. These cells, despite having a general organization similar to that described for cells of the anterior region, showed several distinctive features (Fig. 9A). The most characteristic feature related to the nucleus. It was located in the distal cytoplasm, at about the same level as that of the cells of the anterior region (Fig. 9A). Nevertheless, the nucleus contained an electron-dense structure of rhomboid shape in longitudinal section. This intra-nuclear structure, which was not membrane-bound, measured up to 3 μm long and 1 μm wide, occupying a large portion of the nuclear space (Fig. 9A,B). Diverse sections revealed this intra-nuclear structure to be made up of two or more

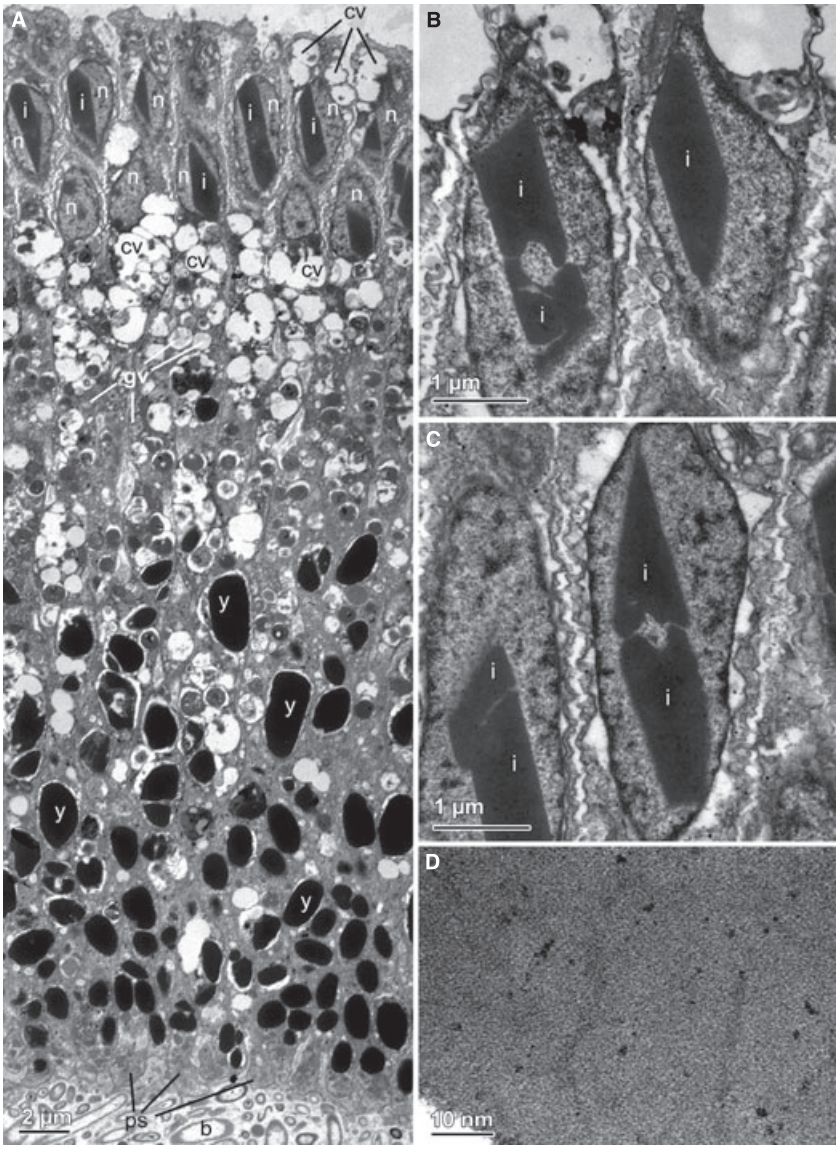

Fig. 9. Cells of the medial region. (A) General view of all cells. The nucleus (n), located below the distal surface, contains a large, rhomboid, electron-dense structure (i). Most electron-clear vesicles (cv) occupy the mid cytoplasm below the nucleus, but in those cells that delimit the anterior larval region (to the left of the micrograph), the electron-clear vesicles also occur above the nucleus. The proximal cytoplasm of the cell is filled with yolk bodies (y) and diverse vesicles with granulose contents (gv). The proximal cell surface emits small pseudopodia (ps) and delimits the internal cavity, which is filled with bacteria (b) and collagen fibrils. (B,C) Details of the nucleus of medial cells showing that the intra-nuclear structure (i) may consist of one or more subunits. (D) Detail of the nuclear structure showing a microgranulose amorphous substructure rather than a paracrystalline pattern, as it could correspond to massive RNA accumulations.

subunits (Fig. 9B and C), depending on the cell. The exact nature of the intra-nuclear material remained unclear (see Discussion), though visualization under high magnification revealed a microgranulose (Fig. 9D) rather than paracrystalline substructure. The amount of yolk in cells of the medial belt was somewhat less than that in cells of the anterior region (Fig. 9A *versus* 8A), occupying only about the proximal half of the cell. In contrast, electron-clear vesicles were comparatively more abundant (Fig. 9A *versus* 8A). It is worth noting that, in most cells, the electron-clear vesicles occupied the central portion of the cell, just below the nucleus (Fig. 9A). Nevertheless, those cells of the medial belt that were located closer to the anterior region had some electron-clear vesicle above the nucleus, as is typical in the cells of the anterior larval region (Fig. 9A).

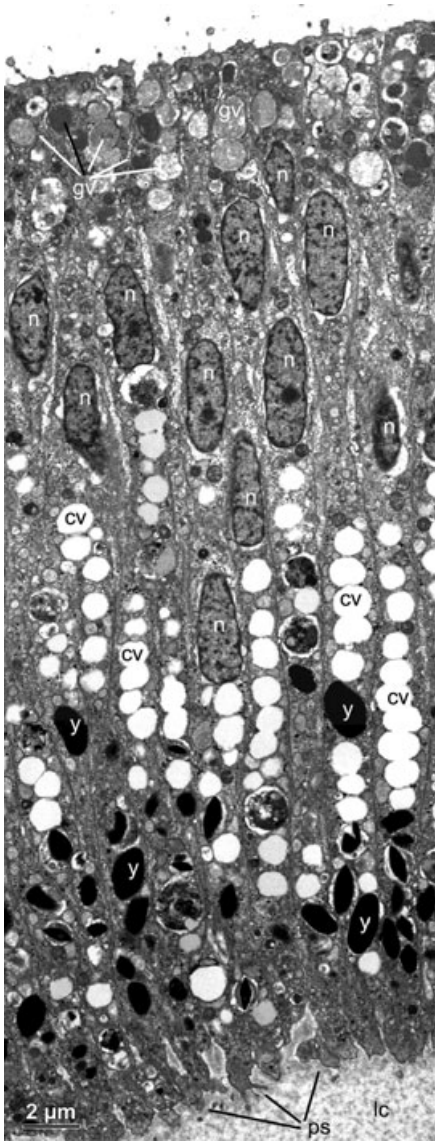

Fig. 10. General view of all cells of the posterior larval region. The distal cytoplasm was filled with vesicles of granulose content (gv), the medial cytoplasm occupied by the nuclei (n), and the proximal cytoplasm contained electron-clear vesicles (cv) and yolk bodies (y). Pseudopodia (ps) are formed at the proximal cell surface. Collagen fibrils were abundant at the larval cavity (lc).

The posterior region of the larval epithelium was made up of cells with scarce yolk bodies, which were consistently located in the most proximal cytoplasm (Fig. 10A). The central portion of the cytoplasm was occupied by rows of fusing electron-clear vesicles. The nucleus, which lacked intra-nuclear bodies, was located in the distal cytoplasm, but slightly deeper than that of cells of the anterior and medial larval regions (Fig. 10A). The distal-most portion of the cells contained membrane-bound vesicles charged with moderately electron-dense materials of both granulose and fibrous aspect.

Therefore, there was a patent anterior–posterior larval gradient in the distribution of the electron-clear vesicles and yolk bodies within the cells. A decrease in yolk content occurred as cells got closer to the posterior pole. Nevertheless, although cells at the anterior, medial, and posterior larval region showed traits distinct from each other, they also shared many features. Nearly all cells of the larval epithelium were monociliated (see Discussion). Differences in the substructure of the proximal axoneme and associated organelles were not detected between cilia of different larval regions. The ciliary insertion was located at the distal cell surface and never took place within a ciliary pit (Fig. 11A). The axoneme arose from the distal ends of the microtubules of a principal centriole or basal body (Fig. 11A). This principal centriole was laterally connected to a simple, electron-dense basal foot, from which numerous microtubules radiated into the adjacent cytoplasm in all directions (Fig. 11B,C). At the distal edge of the principal centriole, nine alar sheets radiated to contact the distal plasmalemma at their corresponding anchoring points (Fig. 11E). An accessory centriole occurred below the principal centriole, being oriented perpendicular to the former (Fig. 11B, D). The accessory centriole showed neither radiating alar sheets nor anchoring points. More interestingly, it gave rise to a short (about 2 μm long), cross-striated ciliary rootlet (Fig. 11D). The cross-striated pattern showed 21-nm band periodicity. The rootlet run parallel to the longitudinal axis of the cell, being consistently located between the nucleus and the Golgi apparatus, which typically oriented its cisternae parallel to the longitudinal axis of the cell (Fig. 11D).

The ciliated cells showed not only a marked proximal–distal organization, but also a subtle anterior–posterior polarization, as the basal foot was consistently located at the 'external'-anterior side of the principal centriole

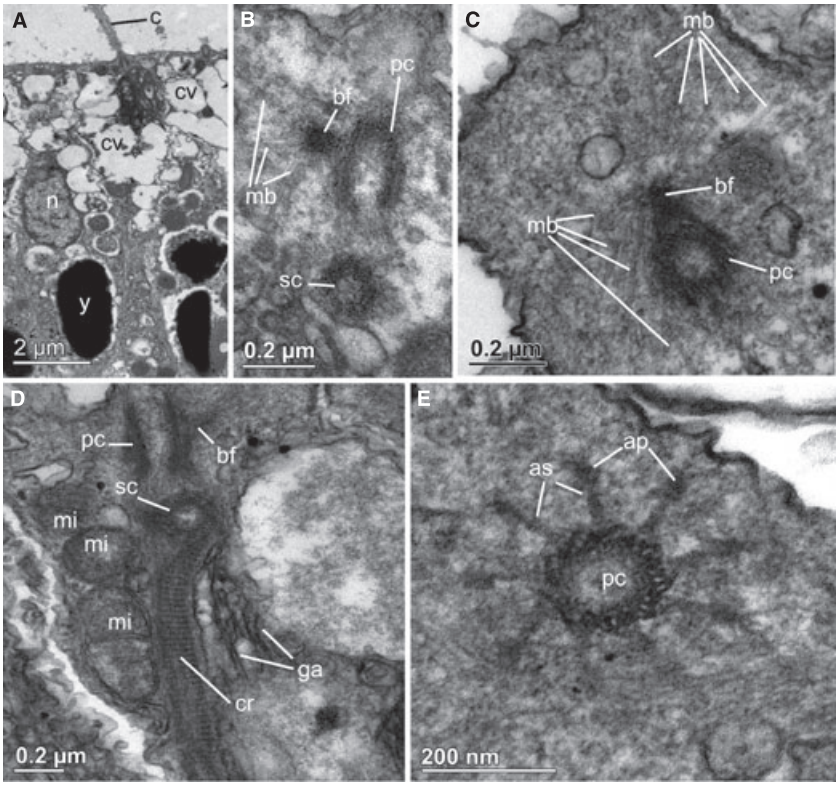

Fig. 11. The basal body and associated structures of the monociliated cells. (A) General view of the cilium (c) insertion at the distal surface of a cell of the anterior larval pole (n = nucleus, cv = electron-clear vesicle, y = yolk body). (B,C) The basal body consisted of a principal centriole (pc), a basal foot (bf) from which microtubules radiated (mb), and an accessory centriole (sc). (D) Detail of a basal body showing the principal centriole (pc), the basal foot (bf), and the accessory centriole (sc) from which a cross-striated ciliary rootlet (cr) arose. The rootlet ran between the Golgi apparatus (ga) and several mitochondria (mi). (E) Cross-section of a principal centriole (pc) at the level of the transition with the axoneme. It shows the nine radiating alar sheets (as) and their respective anchoring points (ap).

(Fig. 11B,C) and the Golgi apparatus at the 'internal'-anterior side of the ciliary rootlet, in front of the nucleus, which was consistently located at the posterior side of the ciliary rootlet (Fig. 11D).

Another noticeable feature shared by all the ciliated cells of the larval body wall was the occurrence of special intercellular junctions at distal and proximal regions of the lateral cell surfaces (Fig. 12A–C). At those regions, the cell membrane became thicker and more electron-dense. More importantly, distal junctions had septae in the intercellular space, being regularly spanned at about 15-nm intervals (Fig. 12B).

In addition to yolk bodies and electron-clear and granulose vesicles, all cells contained abundant small mitochondria around the nucleus (Fig. 12D), as well as abundant glycogen granules in the medial and proximal cytoplasm (Fig. 12E).

The proximal cell surface usually, but not always, formed pseudopodia that protruded into the larval cavity. These pseudopodia were less evident for cells at the anterior and medial region (Figs 8A and 9A) than for those at the posterior pole (Figs 10A and 13C). The larval cavity was filled with abundant bacteria (Figs 6A, 8A and 9A) and collagen fibrils (Figs 10 and 13A–C). Neither phagocytosed bacteria nor symbiotic bacteria were observed within the cytoplasm of the larval cells. Collagen fibrils became denser just below the proximal cell ends, forming a condensation that might be equivalent to a basement membrane (Fig. 13A,B). Nevertheless, fibril condensation did not exist below some cells (Fig. 12C) and it was relatively lax below others (Fig. 13C). Therefore, only at some areas of the larval epithelium did the fibril condensation appear to be a true basement membrane (Fig. 13B) equivalent to that occurring below the choanocyte cell layer of adult *C. candelabrum* (Fig. 13D). In addition to symbiotic bacteria and collagen fibrils, some cellular remains were occasionally found within the larval cavity (Fig. 14), probably material egested by the ciliated larval cells.

Discussion

Reproductive output

The results of the 2-year monitoring of the *C. candelabrum* population, along with those of two previous studies (Riesgo *et al.* 2007a; Riesgo & Maldonado 2008), indicated that fertilization in the studied populations starts sometime in late March, but sperm release extends for several months at the population level so that oocytes are fertilized at very different times during spring. We estimated in a previous study that fertilization success in this species is very high (about 99%) and that very low embryo mortality takes place during development (Riesgo

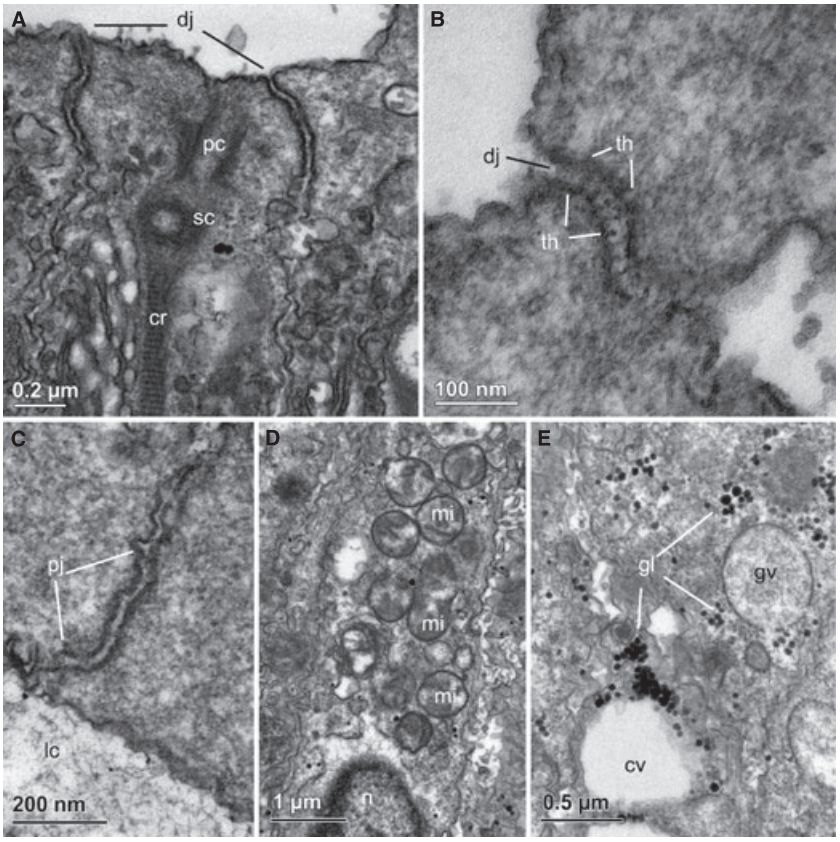

Fig. 12. Cytological features shared by all larval cells. (A) View of the distal cell region showing specialized membrane junctions (dj) at lateral contacts. The centrioles (pc, sc) and the rootlet (cr) of the cilium are also shown. (B) Detail of a distal junction (dj) showing the thickening (th) of the plasmalemma regions involved in the contact and the septate nature of the intercellular space. (C) Detail of a specialized intercellular junction (pj) at proximal cell pole sealing the internal larval cavity (lc). Note that there was not much accumulation of collagen fibrils on the proximal cells surface. (D) Detail of the cytoplasm surrounding the nucleus (n) in which small mitochondria (mi) were often very abundant. (E) Detail of the cytoplasm showing abundant glycogen granules (gl), an electron-clear vesicle (cv), and vesicle (gv) with granulose and fibrous content.

et al. 2007a). Embryogenesis extended for about 3 months at the population level. The first embryos developed very slowly, probably because water temperature was still low. Then the drastic rise in temperature after late spring more or less synchronized embryo development, so that the embryos resulting from the latest fertilization events were finally released only 3 or 4 weeks after the first formed embryos did. There was marked between-year variability in embryo production, with values of embryo density in 2004 nearly doubling those in 2005. Nevertheless, it remains unclear whether such an inter-annual variability was due to natural processes (food availability, failure in fertilization, *etc.*) or to the repetitive monthly tissue removal (about 0.125 cm^3 per sampling) experienced by tagged individuals. It was also found that nearly all individuals of the population (at least those larger than 0.2 cm^3 in volume) were sexually reproductive every year. Because we did not investigate growth rates of early recruits, it remains unclear whether new recruits may achieve that volume during the first year of life and produce gametes, or whether these small gamete-producing individuals result from fission of larger mature individuals. A similar pattern has been reported for the demosponge *Spongia officinalis*, in which fertility also appears to be unrelated to body size (Baldacconi *et al.* 2007).

There are still scarce data about larval output in demosponge populations (*e.g.* Maldonado 2006; Mariani *et al.* 2006; Baldacconi *et al.* 2007; Whalan 2007). Our estimate of the reproductive output of *C. candelabrum*, which was based on a light-microscope study of many sections in 2004 and 2005 and further corroborated by dissection of many individuals under a dissecting microscope in 2006 and 2007 (Fig. 1B), rendered the impressive value of about half a million larvae per m^2 of habitat where this species occurs. This output is even much higher than that recently estimated using a similar methodology for *Crambe crambe* (9375 larvae per m^2 of rocky bottom), which is a spatially dominant species sharing habitat with *C. candelabrum* (Maldonado 2006). The figure estimated for *C. candelabrum* is also far higher than that derived from another previous study by us on *C. crambe* (Uriz *et al.* 1998) using a rougher approach in which embryo counts were not obtained from histological sections but from large, irregular tissue pieces using a dissecting microscope. Such a method probably led to some overestimation, rendering values of approximately 76 embryos per cm^2 of sponge tissue and 30,000 larvae per m^2 of rocky bottom. The moderate abundance of *C. candelabrum* individuals relative to those of the overabundant *C. crambe* (which occupies about 12% of the rocky bottom in the studied

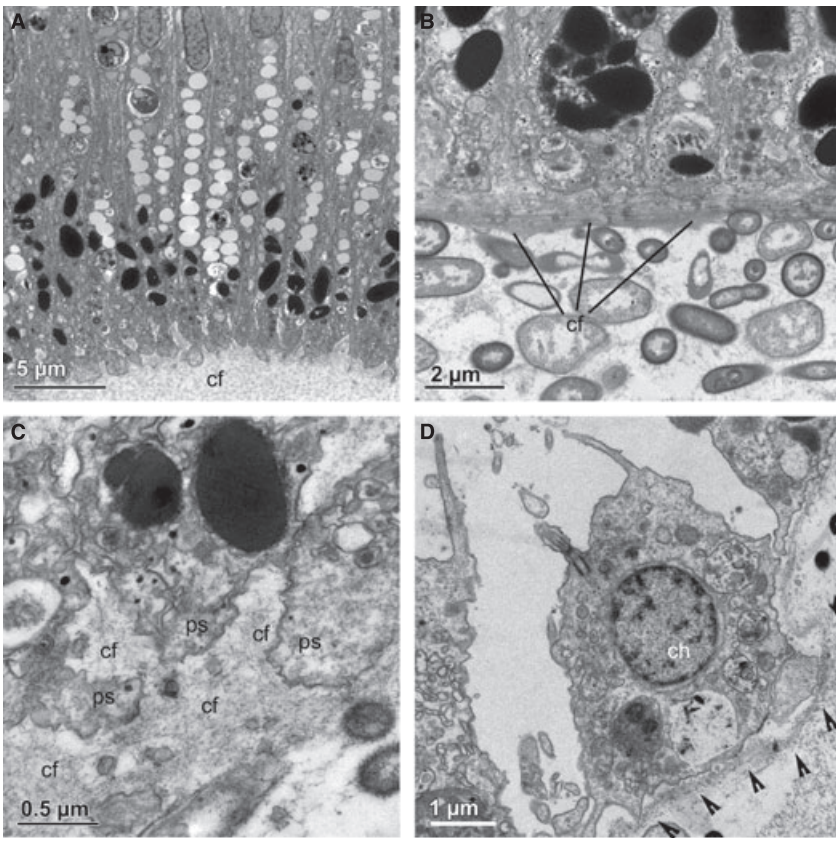

Fig. 13. Collagen reinforcement of epithelial cells. (A) General view of the proximal end of cells at the posterior larval pole, showing abundant collagen fibrils (cf) in the larval cavity, but no marked condensation against the plasmalemma. (B) A very evident condensation of collagen (cf) fibrils (similar to that of a basement membrane) lining the proximal surfaces of cells at the anterior larval pole. (C) Detail of a moderate condensation of collagen fibrils (cf) between the pseudopodia (ps) of the proximal plasmalemma of cells at the anterior larval pole. (D) View of the basement membrane (arrows) occurring below the choanocyte (ch) cell layer of the adults of *Corticium candelabrum*.

communities) may be related to differences in the survival abilities of their larvae and early juveniles.

We detected a strong patchiness in the distribution of adult *C. candelabrum* derived from the discontinuity in the suitability of the environmental benthic conditions, with most individuals being agglomerated at overhangs and shaded rocky walls and clear avoidance of unsuitable light-exposed and silt-exposed substrata. In addition, we also detected a strong patchiness apparently unrelated to microhabitat suitability, as this sponge was quite abundant at shaded walls and overhangs of some sites but completely absent from relatively close sites that provided nearly identical microhabitat conditions. Strong similarity in the general faunal and macroalgal cover between these sponge-populated and non-populated sites supported the idea that they both offered nearly identical microhabitat conditions for the sponge. Such a between-site difference in *C. candelabrum* abundance may well result, among other things, from either philopatric recruitment or local hydrodynamic patterns that favor the concentration of larvae at particular sites. Given that larvae showed no obvious photoresponse in preliminary laboratory experiments, it could not be discarded that larvae settle unselectively on the substrata, so that only those settling at the suitable habitat around the adults would have some chances of recruitment. If unselective settlement is the case, the pattern of adult distribution is expected to be maintained by processes related to post-settlement mortality. An unselective settlement would also account for the high larval outputs of this sponge, needed to deal with substantial losses by larvae being washed out to unsuitable habitats. Further field observations on settlement and survival of juveniles are required to clarify this ecological aspect.

According to tissue sections, larval release was highly asynchronous at the population level, with larvae being released for about 1.5 months, coincidentally with high seawater temperatures. Such a release pattern indicates that moon cycles, tidal forces, and other environmental stimuli known to act as cues that induce a co-ordinate massive larval release in sponge populations are not operating in *C. candelabrum*. The asynchronous larval release may be a strategy to decrease the risk of releasing the entire brood under very unfavorable conditions. A previous study, in which no histological monitoring of the brooding individuals was conducted, reported that larval release in this species takes place synchronously during a few days at the end of July (De Caralt *et al.* 2007). There are two possible interpretations for this apparent discrepancy. Perception of massive synchronous release may derive from field inspection of sponges during days of maximum release at the population level. This method is

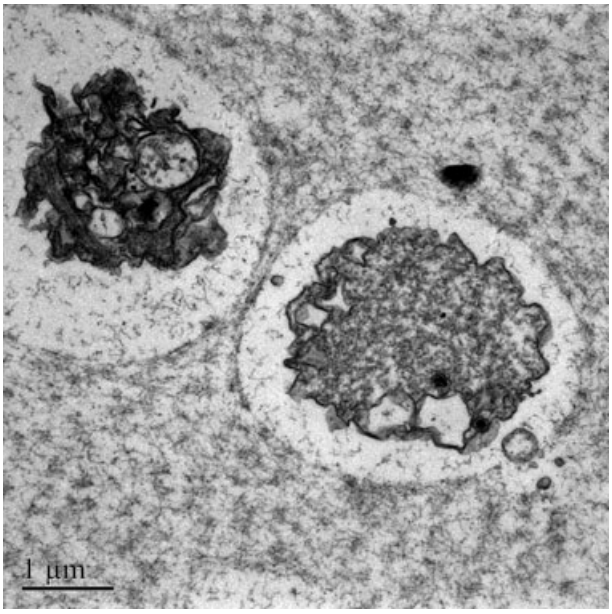

Fig. 14. Cellular remains, probably exocytosed from the larval cells, surrounded by collagen fibrils in the larval cavity.

likely to overlook the slow, little obvious larval outflow extending for several weeks prior to and after the most evident peak of release in the population, as revealed by the histological sections. Alternatively, we cannot discard the idea that the pattern of release may vary from year to year, depending on how climate conditions synchronize processes of gametogenesis and embryo development.

The rate at which larvae were released by the individuals remains unascertained. Indeed, we never observed a massive larval release, only ejection of very few, isolated larvae by some individuals. Although a few sponge species are known to release an important amount of larvae in just a few hours, others appear to use the opposite mechanism. For instance, a local North Atlantic population of *Ophlitaspongia seriata* was estimated to release just 18 larvae per m^2 per day during the release season (Fry 1971). Likewise, individuals of an Apulian population of *S. officinalis* were estimated to release from 25 to 261 larvae per individual and day, depending on the specimen (Baldacconi *et al.* 2007). Therefore, we suspect that in *C. candelabrum* either (i) there is no massive release but just asynchronous release at the individual level or (ii) massive larval releases take place in the afternoon or during night time. Although many demosponges are known to release their larvae early in the morning (reviewed by Maldonado 2006), some do it in the afternoon (*e.g.* Whalan 2007). Larval release during night time may decrease the impact of visual predators or specialized predators that are less active at night. Nevertheless, if larvae are to be released at night, photoreceptors should occur in either mother sponges or larvae to interpret light conditions correctly for release. Such photoreceptors have not being identified so far. Furthermore, the free-swimming larva of *C. candelabrum* did not show marked photoresponses to a variety of light cues used in the laboratory. Nevertheless, occurrence of a photokinesis, which involves neither directional swimming respective to a light source nor obvious photoreceptory organelles, has never been explored in these larvae. It could help to explain massive recruitment in shaded habitats. Being negatively photokinetic, larvae of some demosponges experience a decrease in velocity of the ciliary beating when entering a shaded area from a well-lit area (Maldonado *et al.* 1997). This mechanism favors longer stays in shaded habitats for substratum exploration and eventual settlement.

Previous work on gametogenesis of this sponge uncovered a finely tuned process to maximize success in gamete usage, fertilization, and embryo production (Riesgo *et al.* 2007a). Although our current research corroborates such a high efficiency in embryo production, our estimates of adult abundance and distribution suggest that the efficiency in embryo production and larval output does not directly translate into comparative high levels of adult abundance in the field. We hypothesize that high larval outputs are required to compensate for both serious larval losses during dispersal and substantial juvenile mortality resulting from unselective settlement. Further work on larval dispersal and survival of early settlers is required to elucidate the fate of the reproductive output and to obtain a complete understanding of the life cycle and population dynamics of this sublittoral sponge.

Larval histology

The cytological study of these larvae supported the absence of any recognizable sensorial structures. We only detected monociliated cells. It has long been suggested that the intra-nuclear structures of the medial monociliated cells could somehow be involved in sensory abilities (Meewis 1938), although no further evidence to support such postulation has ever been found. Rather, the granulate substructure of these intra-nuclear structures – which had traditionally been described as paracrystalline – suggests that they could be RNA accumulations, similar to those reported from the nucleus of other sponge cells (Garrone 1969). The unciliated, flask-shaped cells interspersed among the ciliated cells of the larval body wall reported in other studies (*e.g.* Meewis 1938; Lévi & Porte 1962; Boury-Esnault *et al.* 2003; De Caralt *et al.* 2007) were not found in our *C. candelabrum* larvae despite intense sectioning effort, which indicates that they must be quite scarce. Nevertheless, there is no cytological trait in those cells (see Boury-Esnault *et al.* 2003; De Caralt *et al.* 2007) to postulate or suspect any sensorial role. The

flask cells have been tentatively interpreted to have a secretory role (Lévi & Porte 1962). It has also been postulated that many of the electron-clear vesicles occurring at the distal portion of the ciliated cells in the anterior larval pole are secretory, releasing a substance involved in larval attachment (Lévi & Porte 1962). In the posterior larval pole, these electron-clear vesicles concentrate in the proximal portion of the cells, showing an anterior–posterior larval gradient in the distribution of vesicles within the cells. There was also a patent anterior–posterior larval gradient in the distribution of yolk, with yolk content decreasing as cells got closer to the posterior pole. It remains unclear whether this distribution pattern was caused by differential yolk allocation to cells during the embryonic development or by greater yolk metabolic consumption by the cells of the posterior pole.

Observations on living larvae through the compound microscope apparently suggested that the cilium in the cells of the posterior larval pole was longer than in those of the remaining larval body (Fig. 6A,B). In contrast, Boury-Esnault *et al.* (2003) and De Caralt *et al.* (2007) described equally long cilia through the larval body of this larva using SEM observations. It may be that the cilia of the posterior pole are bent in swimming larvae, which would make them to look shorter even if they are not. In the current stage of knowledge, it is hard to decide whether all homosclerophorid species have a larva characterized by equally long cilia – as suggested by Boury-Esnault *et al.* (2003) and De Caralt *et al.* (2007) – or whether some may have cilia of unequal length – as suggested by Barrois (1876), Meewis (1938), and Bergquist *et al.* (1979). As a posterior tuft of longer cilia in other sponge larvae appears to favor maneuverability and acceleration (*e.g.* Maldonado & Young 1996; Maldonado 2006), equal-length cilia through the body (or shorter posterior cilia, if finally demonstrated for some species) might allow restricted maneuverability of the homosclerophorid larva when compared to that of other larval types. Observations on larval behavior in the field revealed that larvae were usually drifting with the anterior pole directed upwards rather than swimming directionally. Such a dispersal mode is also highly consistent with the shape of their body at low Reynolds numbers, which is more suitable for drifting 'upright' than for active 'horizontal' swimming (Maldonado 2006).

It is also noteworthy that the root of the cilium was cross-striated. Such a feature is common in larval cilia of calcareous sponges (*e.g.* Amano & Hori 1992, 2001). It has also been reported in Demospongiae for the monociliated cells of the larva of homosclerophorids (*e.g.* Boury-Esnault *et al.* 2003) and the poecilosclerid *Mycale contarenii* (Lévi 1964), the embryonic monociliated cells – but not larval cells – of the halisarcid *Halisarca dujardini* (Gonobobleva 2007), and the multi-ciliated larval cells of the poecilosclerid *Asbestopluma occidentalis* (Riesgo *et al.* 2007b). Striation periodicity in the rootlet of the larva of *C. candelabrum* was 21 nm, in the larva of *A. occidentalis* it was 29 nm, and in the larva of *M. contarenii* and embryos of *H. dujardini* 50 nm. Yet the short striated ciliary rootlet in *Corticium* and other homosclerophorids is distinct. It does not arise from the principal centriole but from the accessory centriole (Figs 11D and 12A). This unconventional pattern – never before seen in other sponge groups – also occurs in the choanoflagellate *Monosiga ovata*, from which a short striated rootlet of unreported band periodicity has been described as arising from the accessory centriole (Karpov & Leadbeater 1998). Because most investigated choanoflagellates lack a rootlet system, we have still to unravel the potential phylogenetic signal contained in this organelle. Nevertheless, it appears that the hypothesis that *Monosiga*-related choanoflagellates and homosclerophorid sponges could have had some evolutionary connection may deserve some attention and further investigation. From a functional point of view, the ciliary rootlets of this larva are unlikely to be involved in any sensory process. There is now general agreement that the ciliary rootlet of eukaryotic cells, built up of homopolymeric rootletin protofilaments bundled into thicker filaments, is a cytoskeleton anchoring and providing support to cilia, be they motile, sensory or primary (Yang *et al.* 2002, 2005).

Another interesting cytological feature of this larva is the occurrence of special intercellular junctions at the distal cell ends, containing septae in the intercellular space. Deficient fixation that led to obscuration of ultrastructural details probably caused these junctions to be tentatively interpreted as 'zonula adherens' in a previous study of the *C. candelabrum* larva (De Caralt *et al.* 2007). It is worth noting that although septae had not been explicitly reported from other homosclerophorid larvae so far, septation was visible in micrographs of junctions of other homosclerophorids (as noticed by Eerkes-Medrano & Leys 2006), which were originally interpreted as desmosomes by Boury-Esnault *et al.* (2003). Similar septate 'desmosome-like' junctions are known to occur at the distal intercellular contacts in planulae of several scyphozoans and have been described under the name of septate desmosomes (Martin & Chia 1982). Junctions with septae were first reported in Porifera from several calcareous sponges (Ledger 1975; Green & Bergquist 1979). They were also shown in the glass sponge *Rhabdocalyptus dawsoni* (Mackie & Singla 1983). In Demospongiae, they have previously been reported in *Hippospongia communis* (Pavans de Ceccatty *et al.* 1970). From the available evidence, it remains unclear whether these septate desmosome-like junctions of Porifera are simply a special desmosome type or junctions homologous to the septate sealing junctions of higher animals.

Dense accumulation of collagen fibrils has been reported below the ciliated larval epithelium in several homosclerophorids and regarded as a true basement membrane (Boury-Esnault *et al.* 2003) similar to that demonstrated for adult homosclerophorids (Boute *et al.* 1996). To date, a true basement membrane has only been demonstrated for homosclerophorid sponges, although subepithelial reinforcements may occur in other sponges, as suggested by the collagen plexus noticed underneath the larval epithelia of *C. crambe* (*e.g.* Maldonado 2004). Our findings advise caution in interpreting larval collagen in Homosclerophorida as a true basement membrane. We noticed that fibril condensation occurred at some larval regions (Fig. 13B), being quite lax (Figs 10, 13A,C) in others, and even virtually absent from another regions (Fig. 12C). Furthermore, a similar pattern can be noticed in pictures from *Plakina trilopha* published by Boury-Esnault *et al.* (2003, p. 196: fig. 25), in which collagen fibrils were absent below some larval cells, revealing the need for further research and discussion on this issue. A possible explanation is that homosclerophorid larvae may not have a true basement membrane, collagen fibrils simply occurring at a higher density under the epithelial larval cells because these cells are the ones elaborating and exocytosing the fibrils to the larval cavity. In addition, centrifugal forces developed during larval rotation may also facilitate accumulation of fibrils against the proximal cell surfaces lining the internal larval cavity. Likewise, the distribution of vertically transmitted bacteria within the larval cavity also appears to be subject to the forces generated within free-swimming larvae. After fixation, bacteria are seen accumulated at the anterior regions of the larval cavity in some larvae, whereas they occur at the posterior region in others. We suspect that this shift in their location is artifactual and that, in free-swimming larvae, bacteria are suspended in the fluid matrix of the larval cavity, although concentrated at the posterior pole, as indicated by a darker coloration in living larvae. Bacteria and collagen fibrils are expected to sediment through the fluid of the larval cavity once larvae are killed, accumulating at one site or another depending on the orientation of the larva in the embedding medium for microscopy.

Embryological interpretation of the larval stage

Previous studies suggested the hollow larva of homosclerophorids to be a coeloblastula (Ereskovsky & Boury-Esnault 2002; Boury-Esnault *et al.* 2003). Nevertheless, our histological observations indicate that the larva of *C. candelabrum* cannot be regarded as a blastula. Cleavage gave rise to a solid late-stage blastula (stereroblastula) characterized by many small unciliated blastomeres. Because hollowing by centrifugal migration of the blastomeres took place at a late blastula stage (Fig. 7), it cannot be considered to be part of the cleavage process anymore. Furthermore, as soon as the internal blastomeres migrated to organize the embryonic epithelium, they became columnar, polarized cells, which started secreting an intercellular matrix through their proximal surface and differentiated a cilium at their distal surface (Fig. 7). These epithelial cells should not be considered blastomeres anymore, because blastomeres, by definition, are non-differentiated cells. More importantly, the cavity resulting from the hollowing, which started opening at a late-stage blastula, should never be interpreted as a primary blastocoel. By definition, a primary blastocoel should arise directly from cleavage and not from subsequent extensive cell reorganization in the late-stage blastula. Rather, as noticed previously by Maldonado (2004), the process of cell rearrangement looks very much like the process of gastrulation in the remaining animals, which also takes place after cleavage, becoming the first step in cell differentiation. Although gastrulation has long been considered a distinctive embryonic process in all animals (Eumetazoa) except the Porifera, a few independent studies have suggested the occurrence of gastrulation in diverse Porifera groups (*e.g.* Lévi 1956; Efremova 1997; Boury-Esnault *et al.* 1999; Leys & Degnan 2002; Leys 2004; Maldonado 2004; Jenner 2006), urging the need for a search for homologies between the embryology of Porifera and that of the remaining animals.

So far, the 'blastula' suffix in the names 'calciblastula' for the larva of calcinean sponges, 'amphiblastula' for the larva of calcaronean sponges, and 'clavablastula' for the larva of some tetractinomorphs has been used to designate larvae that are clearly blastulae. The calciblastula larva is a coeloblastular stage with an internal cavity that is a primary blastocoel; gastrulation in this group is postulated to occur by multipolar ingression immediately prior to settlement (Maldonado 2004). The amphiblastula larva is also a coeloblastula with a primary blastocoel formed by epithelial eversion; gastrulation is postulated to occur by epiboly in late-stage larvae (Maldonado 2004). Likewise, the clavablastula is also a coeloblastula, but its blastocoel is mostly obliterated by ingression of maternal cells. Because the late development of the clavablastula is poorly known, the stage at which a putative gastrulation takes place has not been identified yet. Recently, the name 'cinctogastrula' was suggested to designate the larva of homosclerophorids (Maldonado 2006), which should not be called 'cinctoblastula' any longer as it is not a blastula. Authors that do not agree with the idea of gastrulation in Homosclerophorida have not incorporated this terminological shift in their studies (*e.g.* De Caralt *et al.* 2007; Ereskovsky *et al.* 2007). Nevertheless, if the emerging idea of gastrulation in Porifera is embraced – now or in the

future – the terminological change is necessary to reconcile larval names with embryological processes.

Acknowledgements

The authors thank Almudena García and Nùria Cortadellas (Microscopy Service, University of Barcelona) for help with sample preparation for the ultrastructural study. This study was supported by two grants of the Spanish Ministry for Science and Education (MCYT- BMC2002-01228; MEC- CTM2005-05366/MAR).

References

Amano S., Hori I. (1992) Metamorphosis of calcareous sponges. I. Ultrastructure of free-swimming larvae. *Invertebrate Reproduction and Development*, **21**, 81–90.

Amano S., Hori I. (2001) Metamorphosis of coeloblastula performed by multipotential larval flagellated cells in the calcareous sponge *Leucosolenia laxa*. *Biological Bulletin*, **200**, 20–30.

Baccetti B., Gaino E., Sarà M. (1986) A sponge with acrosome: *Oscarella lobularis*. *Journal of Ultrastructure and Molecular Structural Research*, **94**, 195–198.

Baldacconi R., Nonnis-Marzano C., Gaino E., Corriero G. (2007) Sexual reproduction, larval development and release in *Spongia officinalis* L. (Porifera, Demospongiae) from the Apulian coast. *Marine Biology*, **152**, 969–979.

Barrois C. (1876) Embryologie des quelques éponges de la Manche. *Annales des Sciences Naturelles*, **3** (art .11), 1–84.

Bergquist P.R., Sinclair M.E., Green C.R., Silyn-Roberts H. (1979) Comparative morphology and behaviour of larvae of Demospongiae. In: Lévi C., Boury-Esnault N. (Eds), *Biologie des Spongiaires*. C. N. R. S., Paris: 103–111.

Borchiellini C., Chombard C., Manuel M., Alivon E., Vacelet J., Boury-Esnault N. (2004) Molecular phylogeny of Demospongiae: implications for classification and scenarios of character evolution. *Molecular Phylogenetics and Evolution*, **32**, 823–837.

Boury-Esnault N., Jamieson B. (1999) Porifera. In: Adiyodi K.G., Adiyodi R.G. (Eds), *Reproductive Biology of Invertebrates. Progress in Male Gamete Ultrastructure and Phylogeny*. John Wiley and Sons, Chichester: 1–20.

Boury-Esnault N., Efremova S., Bézac C., Vacelet J. (1999) Reproduction of a hexactinellid sponge: first description of gastrulation by cellular delamination in the Porifera. *Invertebrate Reproduction and Development*, **35**, 187–201.

Boury-Esnault N., Ereskvosky A.V., Bézac C., Tokina D.B. (2003) Larval development in Homoscleromorpha (Porifera, Demospongiae): first evidence of a basement membrane in sponge larvae. *Invertebrate Biology*, **122**, 187–202.

Boute N., Exposito J.Y., Boury-Esnault N., Vacelet J., Noro N., Miyazaki K., Yoshizato K., Garrone R. (1996) Type IV collagen in sponges, the missing link in basement membrane ubiquity. *Biology of the Cell*, **88**, 37–44.

De Caralt S., Uriz M.J., Ereskovsky A., Wijffels R. (2007) Embryo development of *Corticium candelabrum* (Demospongiae: Homosclerophorida). *Invertebrate Biology*, **126**(3), 211–219.

Dendy A. (1921) The tetraxonid sponge-spicule: a study in evolution. *Acta Zoologica*, Stockholm, **2**, 95–152.

Eerkes-Medrano D.I., Leys S.P. (2006) Ultrastructure and embryonic development of a syconoid calcareous sponge. *Invertebrate Biology*, **125**, 177–194.

Efremova S.M. (1997) Once more on the position among the Metazoa – gastrulation and germinal layers of sponges. *Berliner Geowissenschaftliche Abhandlungen*, **20**, 7–15.

Elvin D.W. (1976) Seasonal growth and reproduction of an intertidal sponge, *Haliclona permollis* (Bowerbank). *Biological Bulletin*, **151**, 108.

Ereskovsky A.V., Boury-Esnault N. (2002) Cleavage pattern in *Oscarella* species (Porifera, Demospongiae, Homoscleromorpha): transition of maternal cells and symbiotic bacteria. *Journal of Natural History*, **36**, 1761–1775.

Ereskovsky A.V., Tokina D.B., Bézac C., Boury-Esnault N. (2007) Metamorphosis of cinctoblastula larvae (Homoscleromorpha, Porifera). *Journal of Morphology*, **268**, 518–528.

Fry W.G. (1971) The biology of larvae of *Ophlitaspongia seriata* from two North Wales populations. *Fourth European Marine Biology Symposium*, **4**, 155–178.

Garrone R. (1969) Une formation paracristalline d'ARN intranucléaire dans les choanocytes de l'Eponge *Haliclona rosea* O.S. (Démosponge, Haplosclérides). *Comptes Rendus de l'Académie des Sciences, Paris*, **269**, 2219–2221.

Gonobobleva E. (2007) Basal body formation in external flagellated cells of *Halisarca dujardini* larvae (Demospongiae, Halisarcida) in the course of embryonic development. In: Custódio M.R., Lôbo-Hajdu G., Hajdu E., Muricy G. (Eds), *Porifera Research. Biodiversity, Innovation and Sustainability*. Museu Nacional de Rio de Janeiro, Rio de Janeiro: 345–351.

Green C.R., Bergquist P.R. (1979) Cell membrane specialisation in the Porifera. In: Lévi C., Boury-Esnault N. (Eds), *Biologie des Spongiaires*. C. N. R. S., Paris: 153–157.

Heider K. (1886) Zur Metamorphose der *Oscarella lobularis* O Schm. *Arbeiten aus dem Zoologischen Instituten der Universität Wien*, **6**, 175–236.

Hooper J.N.A., Van Soest R.W.M. (2002) Class Demospongiae Sollas, 1885. In: Hooper J.N.A., Van Soests R.W.M. (Eds), *Systema Porifera: A Guide to the Classification of Sponges*. Kluwer Academic/Plenum Publisher, New York: 15–18.

Jenner R.A. (2006) Challenging received wisdoms: some contributions of the new microscopy to the new animal phylogeny. *Integrative and Comparative Biology*, **46**, 93–103.

Karpov S.A., Leadbeater B.S.C. (1998) Cytoskeleton structure and composition in choanoflagellates. *Journal of Eukaryotic Microbiology*, **45**(3), 361–367.

Ledger P.W. (1975) Septate junctions in the calcareous sponge *Sycon ciliatum*. *Tissue and Cell*, **1**, 13–18.

Lévi C. (1956) Étude des *Halisarca* de Roscoff. Embryologie et systématique des Demosponges. *Archives de Zoologie Expérimentale et Générale*, **93**, 1–181.

Lévi C. (1964) Ultrastructure de la larve parenchymella de démosponge. I. *Mycale contarenii* (Martens). *Cahiers de Biologie Marine*, **5**, 97–104.

Lévi C., Porte A. (1962) Étude au microscope électronique de l'éponge *Oscarella lobularis* Schmidt et de sa larve amphiblastula. *Cahiers de Biologie Marine*, **3**, 307–315.

Leys S.P. (2004) Gastrulation in sponges. In: Stern C.D. (Ed.), *Gastrulation. From Cells to Embryo*. Cold Spring Harbor Laboratory Press, Cold Spring Harbor, NY: 23–31.

Leys S.P., Degnan B.M. (2002) Embryogenesis and metamorphosis in a haplosclerid demosponge: gastrulation and transdifferentiation of larval ciliated cells to choanocytes. *Invertebrate Biology*, **121**, 171–189.

Mackie G.O., Singla C.L. (1983) Studies on hexactinellid sponges. I. Histology of *Rhabdocalyptus dawsoni* (Lambe, 1873). *Philosophical Transactions of the Royal Society of London*, **301**, 365–400.

Maldonado M. (2004) Choanoflagellates, choanocytes, and animal multicellularity. *Invertebrate Biology*, **123**, 231–242.

Maldonado M. (2006) The ecology of the sponge larva. *Canadian Journal of Zoology*, **84**, 175–194.

Maldonado M., Bergquist P.R. (2002) Phylum Porifera. In: Young C.M., Sewell M.A., Rice M.E. (Eds), *Atlas of Marine Invertebrate Larvae*. Academic Press, San Diego: 21–50.

Maldonado M., Riesgo A. (2007) Intra-epithelial spicules in a homosclerophorid sponge. *Cell Tissue Research*, **328**, 639–650.

Maldonado M., Young C.M. (1996) Effects of physical factors on larval behavior, settlement, and recruitment of four tropical demosponges. *Marine Ecology Progress Series*, **138**, 169–180.

Maldonado M., George S.B., Young C.M., Vaquerizo I. (1997) Depth regulation in parenchymella larvae of a demosponge: relative roles of skeletogenesis, biochemical changes and behavior. *Marine Ecology Progress Series*, **148**, 115–124.

Maldonado M., Cortadellas N., Trillas M.I., Rützler K. (2005) Endosymbiotic yeast maternally transmitted in a marine sponge. *Biological Bulletin*, **209**, 94–106.

Mariani S., Uriz M.J., Turon X., Alcoverro T. (2006) Dispersal strategies in sponge larvae: integrating the life history of larvae and the hydrologic component. *Oecologia*, **149**, 174–184.

Martin V.J., Chia F.S. (1982) Fine structure of a scyphozoan planula, *Cassiopeia xamachana*. *Biological Bulletin*, **163**, 320–328.

Meewis H. (1938) Contribution à l'étude de l'embryogénèse des Myxospongidae: *Halisarca lobularis* (Schmidt). *Archives de Biologie*, **50**, 3–66.

Muricy G., Díaz M.C. (2002) Order Homosclerophorida Dendy, 1905, Family Plakinidae Schulze, 1880. In: Hooper J.N.A., Van Soest R.W.M. (Eds), *Systema Porifera. A Guide to the Classification of Sponges*. Kluwer Academic/Plenum Publishers, New York: 71–82.

Muricy G., Bézac C., Gallissian M.F., Boury-Esnault N. (1999) Anatomy, cytology and symbiotic bacteria of four Mediterranean species of *Plakina* Schulze, 1880 (Demospongiae, Homosclerophorida). *Journal of Natural History*, **33**, 159–176.

Nichols S.A. (2005) An evolution of support for order-level monophyly and interrelationships within the class Demospongiae using partial data from the large subunit rDNA and cytochrome oxidase subunit I. *Molecular Phylogenetics and Evolution*, **34**, 81–96.

Pavans de Ceccatty M., Thiney Y., Garrone R. (1970) Les bases ultrastructurales des communications intercellulaires dans les oscules de quelques éponges. *Symposia of the Zoological Society of London*, **25**, 449–466.

Reynolds E.S. (1963) The use of lead citrate at high pH as an electron opaque stain in electron microscopy. *Journal of Cell Biology*, **17**, 208–212.

Riesgo A., Maldonado M. (2008) Differences in reproductive timing between sponges sharing habitat and thermal regime. *Invertebrate Biology*, **128**, in press. doi: 10.1111/j.1744-7410.2008.00128x.

Riesgo A., Maldonado M., Durfort M. (2007a) Dynamics of gametogenesis, embryogenesis, and larval release in a Mediterranean homosclerophorid demosponge. *Marine and Freshwater Research*, **58**, 398–417.

Riesgo A., Taylor C., Leys S. (2007b) Reproduction in a carnivorous sponge: the significance of the absence of an aquiferous system to the sponge body plan. *Evolution and Development*, **9**, 618–631.

Ros J., Romero J., Ballesteros E., Gili J.M. (1985) Diving in blue water. In: Margalef R. (Ed.), *Western Mediterranean*. Pergamon, Oxford: 233–295.

Schulze F.E. (1880) Untersuchungen über den Bau und die Entwicklung der Spongien. Die Plakiniden. *Zeitschrift für Wissenschaftliche Zoologie*, **34**, 407.

Tuzet O., Paris J. (1964) La spermatogenèse, l'ovogenèse, la fécondation et les premiers stades du développement chez *Octavella galangaui* Tuzet et Paris. *Vie et Milieu*, **15**, 309–327.

Uriz M.J., Maldonado M., Turon X., Martí R. (1998) How do reproductive output, larval behaviour, and recruitment contribute to adult spatial patterns in Mediterranean encrusting sponges? *Marine Ecology Progress Series*, **167**, 137–148.

Wang X., Lavrov D.V. (2007) Mitochondrial genome of the homoscleromorph *Oscarella carmela* (Porifera, Demospongiae) reveals unexpected complexity in the common ancestor of sponges and other animals. *Molecular Biology and Evolution*, **24**, 363–373.

Whalan S. (2007) *Reproduction, larval dispersal, and population genetics of the sponge* Rhopaloeides odorabile. Ph.D. Dissertation, James Cook University, Townsville. 536pp.

Yang J., Liu X., Yue G., Adamian M., Bulgakov O., Li T. (2002) Rootletin, a novel coiled-coil protein, is a structural component of the ciliary roolet. *Journal of Cell Biology*, **159**, 431–440.

Yang J., Gao J., Adamian M., Wen X., Pawlyk B., Zhang L., Sanderson M.J., Zuo J., Makino C.L., Li T. (2005) The ciliary rootlet maintains long-term stability of sensory cilia. *Molecular and Cellular Biology*, **25**, 4129–4137.